Computational Physics - FYS3150 Project 4

Håvard Sinnes Haughom and Ida Risnes Hansen

Nov 18, 2019

Abstract

The two-dimensional Ising model with square lattices is implemented and tested for lattice sizes from $20x20$ up to $100x100$, using the Metropolis algorithm. The most likely state was reached after 10^6 Monte Carlo cycles. We estimate the critical temperature for the different lattice sizes. Based on these, we approximate the critical temperature for an infinite lattice, $T_C(L = \infty) \approx 2.269$.

1 Introduction

Many of the properties of ferromagnetic materials can be described using the Ising model, developed by Ernst Ising. It is characterized by a lattice of atoms described by some binary property, for example spin up or down. With this, we can study various statistical properties of the material, and how these change with temperature. In particular, we can look for characteristic behavior around the critical temperature for phase transitions to occur.

In this project, we will use the Metropolis algorithm to estimate the expectation values of energy and magnetisation in a ferromagnetic material, using the two-dimensional Ising model. Based on these, we will then calculate the specific heat per spin and susceptibility per spin of the material.

We will first study the convergence and efficiency of the algorithm. Both by comparison with the known analytical values for small lattices, as well as by finding the necessary number of Monte Carlo cycles to reach equilibrium.

When we are sufficiently confident in the algorithm and its properties, we will qualitatively study changes in the system over temperature. We briefly look at the energy distribution and variance, before we focus on changes in the statistical variables around the critical temperature. By studying the differences for increasing lattice sizes, we finally attempt to approximate the critical temperature as the lattice size becomes big.

2 Theory

2.1 The Ising model

The Ising model places the atoms of a ferromagnetic material in a lattice and assigns them a binary property, commonly spin $s = \pm 1$. For a lattice of N atoms, the energy of a given state i,

$$E_i = -J \sum_{\langle kl \rangle}^{N} s_k s_l, \tag{1}$$

where the notation $\langle kl \rangle$ means the sum is over nearest neighbours and J is the coupling constant from the interaction strength between neighbouring spins. The magnetization is just the sum over all spins,

$$\mathcal{M}_i = \sum_{j=1}^{N} s_j. \tag{2}$$

For a system of N atoms, there is 2^N possible states, as each atom has two possible configurations. In applications, the lattice is always finite, and it is necessary to handle the boundaries. One way is to use

periodic boundary conditions, so that the atom on an edge is counted as the neighbour of the atom on the opposite edge. From this, we can obtain important statistical quantities[1].

2.2 Statistical quantities

The partition function of the system,

$$Z = \sum_{i=1}^{N} e^{-\beta E_i}, \tag{3}$$

while the expectation value for the energy and absolute magnetization is

$$\langle E \rangle = \frac{1}{Z} \sum_{i=1}^{N} E_i e^{-\beta E_i} \qquad \langle |\mathcal{M}| \rangle = \frac{1}{Z} \sum_{i=1}^{N} |\mathcal{M}_i| e^{-\beta E_i}.$$

Their variances

$$\sigma_E^2 = \langle E^2 \rangle - \langle E \rangle^2 \qquad \sigma_{|\mathcal{M}|}^2 = \langle |\mathcal{M}|^2 \rangle - \langle |\mathcal{M}| \rangle^2$$

From this, we can also find the heat capacity and susceptibility,

$$C_V = \frac{\sigma_E^2}{k_B T^2} \qquad \chi = \frac{\sigma_{|\mathcal{M}|}^2}{k_B T}$$

The correlation length, $\xi(T)$, is another important parameter. It is the characteristic scale at which the bulk properties of the material differ from its overall properties[1].

2.3 Phase transitions in the Ising model

Ferromagnetic transitions are continuous, 2nd order phase transitions that occur at critical temperatures T_C where the correlation length diverge,

$$\xi(T) \sim |T_C - T|^{-\nu}.$$

For infinite lattices, C_V and χ diverge as the temperature $T \to T_C$. It is possible to relate properties of finite and infinite lattices,

$$T_C(L) - T_C(L = \infty) \propto L^{-1/\nu}, \tag{4}$$

where L is the dimension of the finite lattice. As we approach the critical temperature, many of the statistical quantities above can be approximated as power laws of $T - T_c$, and thus as power laws of L.

$$C_V(T) \sim |T_C - T|^{-\alpha} \to L^{\alpha/\nu} \qquad \alpha = 0 \tag{5}$$

$$\chi(T) \sim |T_C - T|^{-\gamma} \to L^{\gamma/\nu} \qquad \gamma = -7/4 \tag{6}$$

For finite lattices, we see C_V and χ will not diverge for $T \to T_C$, but display broad maxima that narrows with growing lattice size L[1].

2.4 The Metropolis algorithm for calculating eigenvalues

The Metropolis algorithm is a Monte Carlo Markov Chain method that can be used to calculate expectation values.

Starting from an arbitrary lattice configuration, the idea is to flip an arbitrary spin, but only conditionally accept the new configuration. If the energy change is negative, the configuration is accepted, while an increase in energy is only accepted based on a Boltzmann probability distribution. In other words, increases in energy are more likely accepted at higher temperatures.

This is repeated for N Monte Carlo cycles, for which the state values are cumulatively summed. The final value is then divided by N to get the expectation value[1].

3 Method

We use the two-dimensional, square-lattice Ising model with periodic boundary conditions. All the code for the implementation in C++ can be found in the repository at github.com/HHaughom/FYS3150-Project4.git as well as all the files of data from the runs presented in this report. Only exception are the files from the energy during one simulation that were to big for github.

3.1 Calculating the eigenvalues

We implement the Metropolis algorithm for computing expectation values for energy $\langle E \rangle$, absolute magnetisation $\langle |M| \rangle$, as well as the heat capacity C_V and susceptibility χ. All values are per spin.

We store the spin matrix in a double pointer and give two options for initializing it. One ordered option, where all spins point up ($s = 1$), and one unordered, where the initial orientation is randomized throughout the lattice. We calculate the energy and absolute magnetisation for the initial state, using Equation 1 and 2. While the successive changes in energy and magnetisation are found with

$$\Delta E = -2S_{kl}\left(S_{k,(l+L-1)\%L} + S_{k,(l+L+1)\%L} + S_{(k+L-1)\%L,l} + S_{(k+L+1)\%L,l}]\right)$$
$$\Delta M = 2S_{kl}$$

where S is the spinmatrix, k, l are the indices of the flipped spin, while the syntax $(k + L \pm 1)\%L$ accounts for the periodic boundary conditions.

For simplicity, we set $k_B = J = 1$. The implementation therefore needs to be initialized by a temperature with energy dimension.

3.2 Testing the implementation

We test the implementation for lattice size $L = 2$, for which we have the analytical values (see appendix). We use $N = 10^6$ Monte Carlo cycles and temperature $k_BT/J = 1$.

We compute $\langle E \rangle$ and $\langle |M| \rangle$ for a lattice of size $L = 20$ over increasing Monte Carlo cycles $logN = 1, 2, ..., 8$. We use both an ordered and an un-ordered initial configuration and look at the temperatures $k_BT/J = 1.0$ and $k_BT/J = 2.4$. Here, we note how many cycles are needed before the values stabilize.

Additionally, we count the number configurations that are accepted for each of temperature as a function of Monte Carlo cycles, $logN = 1, 2, ..., 7$. We use a random initial configuration and look at differences in the behavior at the different temperatures.

3.3 Energy probability distribution

Using the computed data for the $L = 20$ lattice, we plot the normalized distribution of the accepted energies for both temperatures $k_BT/J = 1.0$ and $k_BT/J = 2.4$ and compare this to the energy variances.

3.4 Phase transitions and critical temperature

Next, we compute $\langle E \rangle$, $\langle |M| \rangle$, C_V and χ for lattice sizes $L = 20,\ 40,\ 60,\ 80,\ 100$ over the temperature range $T \in [2.0, 3.0]$. We use the step size $dT = 0.005$ and $N = 10^7$ Monte Carlo Cycles.

3.4.1 Parallelization

At this point there are so many computations that it is quite time-demanding. To reduce the time needed we parallelized parts of the code using the *MPI*-library in C++[3]. The parallelized code was run on a computer with 4 CPUs, i.e 4 parallel computations. We measured the performance of the implementation by timing it using the *chrono* library in C++[4]. The code that was run to test it was to calculate $\langle E \rangle$, $\langle |M| \rangle$, C_V and χ for $L = 20, 40, 60, 80$ with and without parallelization.

3.5 Critical temperature for $L = \infty$

For each of the parameters, we look for characteristic changes over the interval, and estimate the critical temperature for each of the lattice sizes. Finally, using Equation 4, we estimate the critical temperature as the lattice size $L \to \infty$ by making a linear fit using the least mean square method.

4 Results

4.1 Convergence for lattice L=2

For the L=2 lattice with $N = 10^6$ Monte Carlo cycles, the results match the analytical values within three significant digits for the energy and magnetisation, two digits for the susceptibility and within one digit for the heat capacity.

	$\langle E \rangle$	$\langle \lvert \mathcal{M} \rvert \rangle$	C_V	χ
Analytical	-1.9960	0.9987	0.032085	0.004005
Numerical	-1.9959	0.9986	0.032385	0.004113

4.2 Expectation values over Monte Carlo cycles

The expectation values for energy and absolute magnetisation become stable after about 10^6 Monte Carlo cycles for the temperature $k_BT/J = 2.4$, and after 10^5 cycles for $k_BT/J = 1.0$. The random and ordered initial states perform similarly, the random being generally better over many runs.

The energy increase with higher temperature, while the absolute magnetisation decrease. It took 0.39 seconds for the implementation to run for 10^6 and 0.06 seconds to run for 10^5 cycles. I.e we have equilibration time of 0.39 seconds at $k_BT/J = 1.0$ and 0.06 seconds at $k_BT/J = 2.4$.

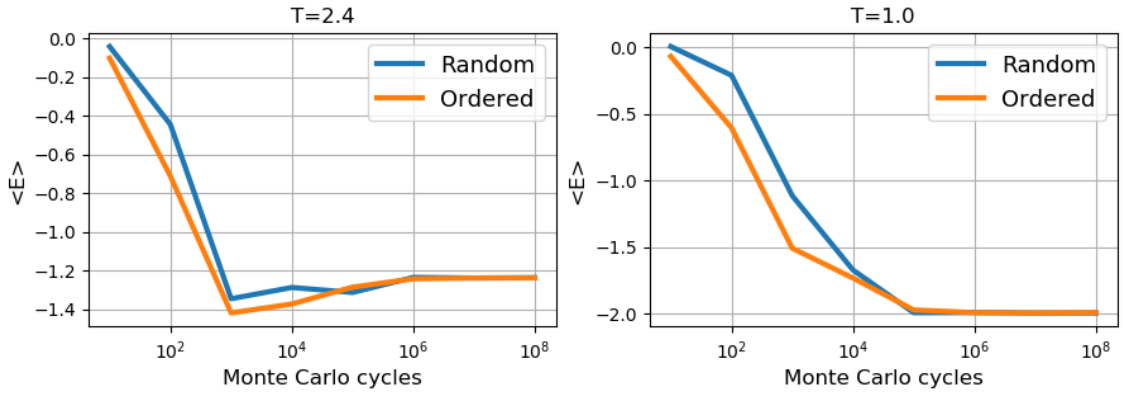

Figure 1: The expectation value of the energy per spin plotted for different number of Monte Carlo cycles at the two temperatures $k_BT/J = 1.0$ and $k_BT/J = 2.4$. Both a random and an ordered initial lattice configuration is used. The lattice size is $L = 20$.

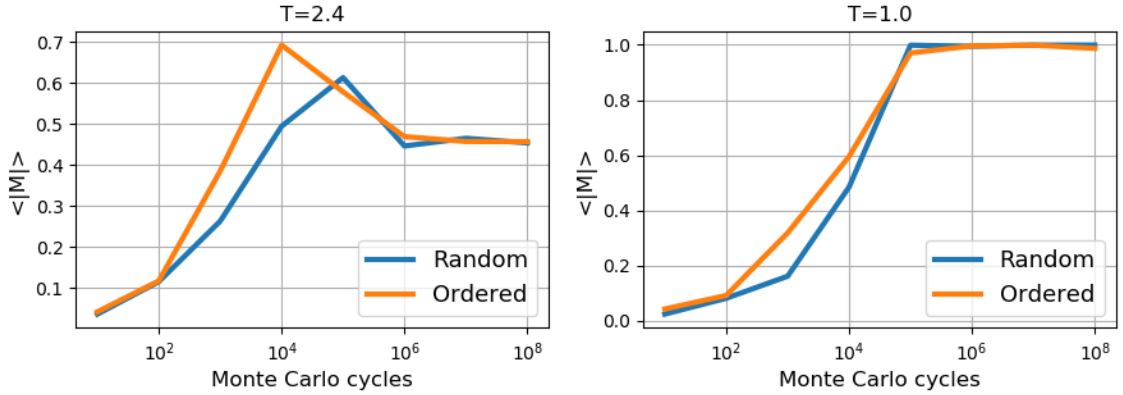

Figure 2: The expectation value of the absolute magnetisation per spin plotted for different number of Monte Carlo cycles at $k_BT/J = 1.0$ and $k_BT/J = 2.4$. A random and an ordered initial lattice configuration is used at both temperatures, and the lattice size is $L = 20$.

The number of accepted configurations decrease over Monte Carlo cycles. The rate at $k_BT/J = 1.0$ decrease rapidly towards zero, while the rate at $k_BT/J = 2.4$ stabilize around 0.25.

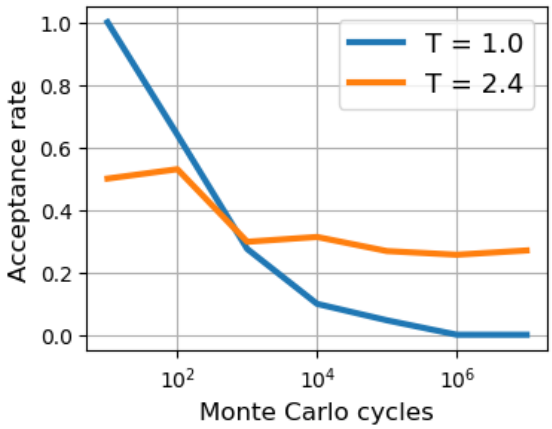

Figure 3: The ratio of accepted energies in the Metropolis algorithm is plotted as a function of total Monte Carlo cycles at the temperatures $k_BT/J = 1.0$ and $k_BT/J = 2.4$. The lattice size is $L = 20$ and random initialisation.

4.3 Energy probability distribution

The energy probability distribution for temperatures $k_BT/J = 1.0$ and $k_BT/J = 2.4$ are shown in Figure 4. The distribution at $k_BT/J = 1.0$ has a very distinct peak at $E = -2.0$ that goes quickly towards 0 and stays there for the other energies. With $k_BT/J = 2.4$ we have a peak at around $E = -1.2$. This peak is not as distinct as for $k_BT/J = 1.0$, but it also goes towards 0 at energies away from the peak.

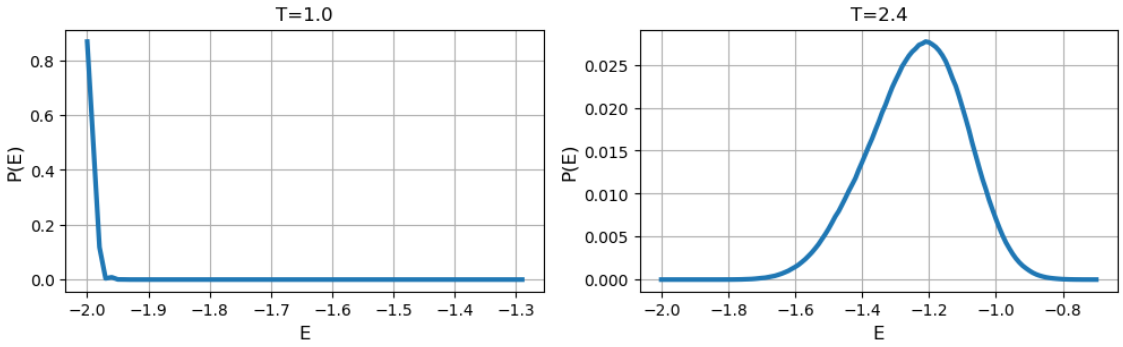

Figure 4: The normalized distribution of accepted energies in the Metropolis algorithm is plotted for $k_BT/J = 1.0$ and $k_BT/J = 2.4$. The data is obtained from a simulation on a lattice with size $L = 20$ with $N = 10^7$ Monte Carlo cycles.

In Figure 5 we have plotted the variance , σ_E, as a function of N Monte Carlo cycles at $k_BT/J = 1.0$ and $k_BT/J = 2.4$. The variance starts out similar for both temperatures at $\sigma_E = 10^{-2}$ and decrease as N increases. The variance at $k_BT/J = 1.0$ decreases faster than the variance at $k_BT/J = 2.4$.

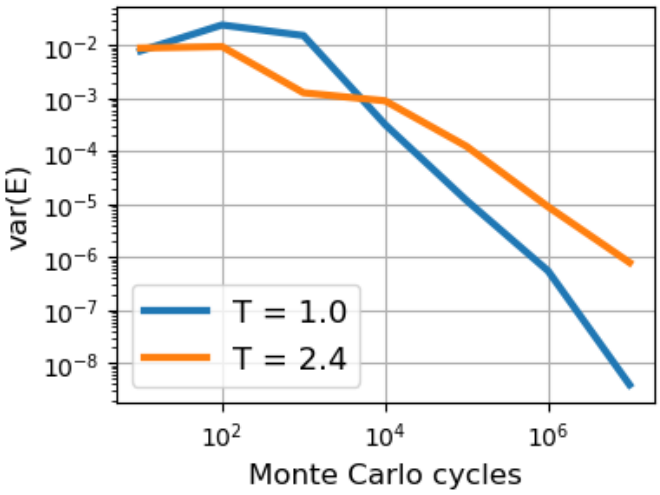

Figure 5: The energy variance plotted over Monte Carlo cycles for $k_BT/J = 1.0$ and $k_BT/J = 2.4$, and lattice size is $L = 20$

4.4 Phase transitions

The expectation values for energy per spin, $\langle E \rangle$, and absolute magnetisation per spin, $\langle |M| \rangle$, as a function of temperature are shown for different lattice sizes in Figure 6.

The energy is increasing with increasing temperature. Specially in the range $k_BT/J = [2.2, 2.4]$. At higher and lower temperatures than this, it is still increasing, but seems to slow down and stabilize at values around $\langle E \rangle \approx -1.8$ for low temperatures and $\langle E \rangle \approx -0.8$ for high temperatures. The energy seems to be almost independent of lattice size.

Similarly to the energy, the magnetisation also has a big change in the range $k_BT/J = [2.2, 2.4]$. At temperatures lower than 2.2 it seems to stabilize at $\langle |M| \rangle \approx 1.0$ and at temperatures higher than 2.4 it stabilizes towards $\langle |M| \rangle \approx 0.0$. The change in magnetisation happens faster for higher lattice sizes, but converges towards the same values independent of lattice size.

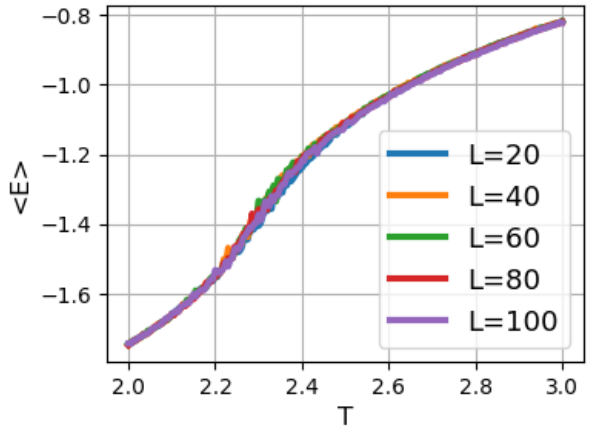

(a) The expectation value of energy per spin.

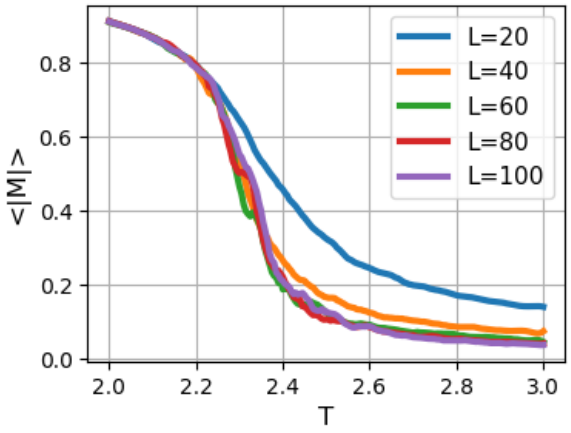

(b) The expectation value of magnetisation per spin. A smoothing function was applied to the data.

Figure 6: The expectation values of energy and absolute magnetisation per spin plotted for lattice sizes $L = 20$, 40, 60, 80, 100 in the temperature range $k_BT/J \in [2.0, 3.0]$. The step size is $dT = 0.005$ and the number of Monte Carlo cycles $N = 10^7$.

In Figure 7 you can see the specific heat capacity per spin, C_V, and susceptibility per spin, χ as a function of temperature for different lattice sizes.

The specific heat capacity per spin starts out at $C_V \approx 0.9$ for all lattice sizes and then goes on to peak at $k_B T/J \approx 2.3$. The peak is higher for bigger lattice sizes with a peak at $C_V \approx 5.9$ for $L = 100$ and a peak at $C_V \approx 1.8$ for $L = 20$. The peaks also seems to be shifted a bit to the right for higher lattice sizes, i.e C_V peaks at higher temperatures for higher lattice sizes. After the peak the specific heat capacity goes down again.

The susceptibility per spin goes from $\chi = 0.0$ up until $k_B T/J \approx 2.3$ where we have a very distinct peak. The peak is, as for specific heat capacity per spin, higher for bigger lattices, with $C_V \approx 150$ for $L = 100$ and $C_V \approx 10$ for $L = 20$. Also similarly to specific heat capacity per spin, it seems to be shifted towards higher temperatures for bigger lattices. After the peak it goes down towards $\chi = 0.0$ again for all lattice sizes.

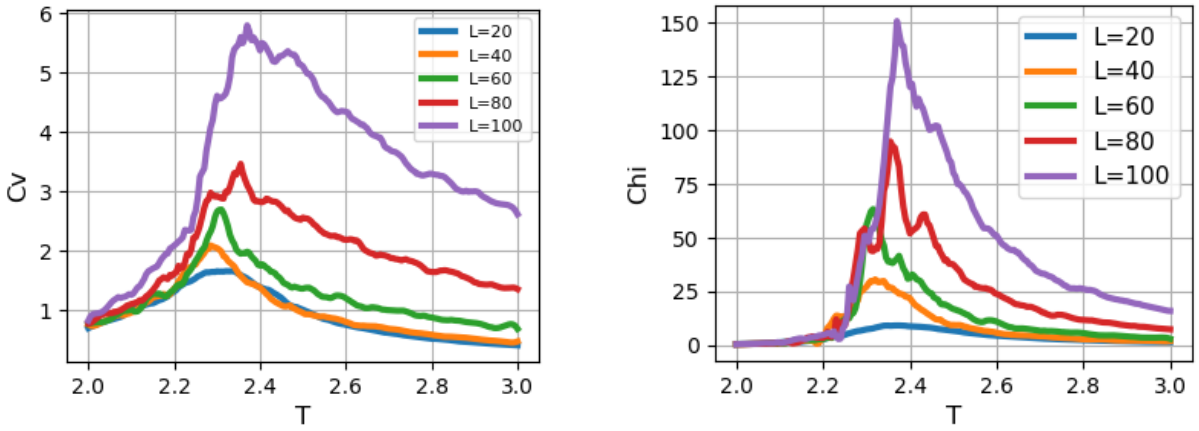

(a) Specific heat capacity per spin.

(b) Susceptibility per spin.

Figure 7: The specific heat and susceptibility per spin plotted for lattice sizes $L = 20$, 40, 60, 80, 100 in the temperature range $k_B T/J \in [2.0, 3.0]$. The step size is $dT = 0.005$ and the number of Monte Carlo cycles $N = 10^7$. A smoothing function was applied to both data sets.

4.4.1 Parallelization

When running the code described in 3.4.1 with parallelization of 4 CPUs we had a total time spent of $t = 94.99$ seconds. Without the parallelization, i.e on 1 CPU we got $t = 259.40$ seconds, both values are taken as mean of five runs. This means that we had a speedup of

$$\text{Speedup} = \frac{259.40s}{94.99s} = 2.73$$

4.5 Critical temperature for $L = \infty$

In Figure 8 we have plotted datapoints corresponding to $L \cdot T_C$ for different lattice sizes and done a least mean squared linear fit. The critical temperature in the thermodynamic limit as $L \to \infty$ is the slope of the linear fit which is $T_C(L = \infty) = 2.42$.

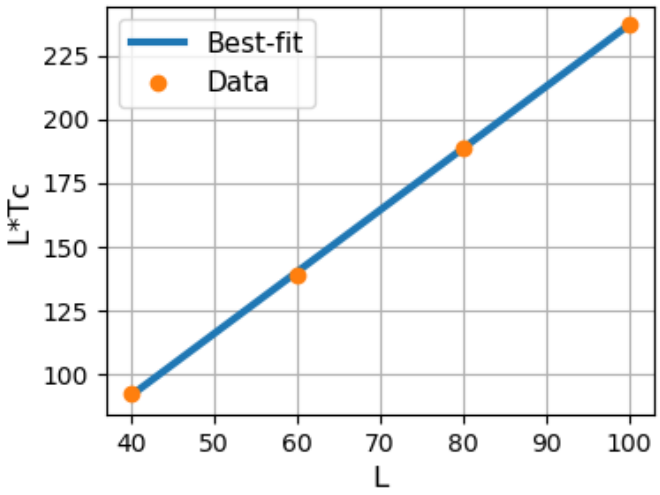

Figure 8: Plot of $T_C(L) \cdot L = T_C(L = \infty) \cdot L + a$ with $\nu = 1$. The datapoints have been found by looking at the plots of $\langle |M| \rangle$, C_V and χ in Figure 6 and 7 and taking the mean of the critical temperature for lattice sizes $L = 40, 60, 80, 100$. We neglected the plot of the energy, since it was hard to estimate the critical temperature there. The linear fit is found by the least mean squared method.

5 Discussion

5.1 Convergence for lattice $L = 2$

To get the numerical values to match the analytical results (see appendix) for the $L = 2$ lattice we needed $N = 10^6$ Monte Carlo cycles. The implementation was timed and used about 0.1 seconds to reach convergence.

5.2 Expectation values over Monte Carlo cycles

The expectation values for energy and absolute magnetisation became stable after $N = 10^5$ cycles for for $k_BT/J = 1.0$ and after $N = 10^6$ cycles for k_BT/J, and the implementation had a equilibrium time of 0.39 seconds for $k_BT/J = 1.0$ and 0.06 seconds for $k_BT/J = 2.4$.

It is expected that the equilibration time is shorter for lower temperatures. With low temperatures the Metropolis algorithm is less likely to accept new configurations because we use a Boltzmann distribution. This means that there will be more fluctuations with higher temperatures, which leads to the need for more Monte Carlo cycles to reach the correct value and stabilize.

In the simulation we also saw that both the ordered and the random initial state performed very similar. We expected the ordered initialisation to perform better at low temperatures, and the random to perform better at high temperatures. This is because at low temperatures the ordered initial state is very similar to the expected final state after the system has converged and stabilized. While the random initialisation is closer to the expected final state at higher temperatures. This would perhaps be clearer if we chose a higher temperature than $k_BT/J = 2.4$ because the critical temperature has been estimated to $k_BT/J = 2.42$. By going above this we would maybe see some clearer distinction between the ordered and random initialisation.

In Figure 3 we see that the acceptance rate is very high initially for $k_BT/J = 1.0$ but it decreases and goes to 0 very fast. While the acceptance rate for $k_BT/J = 2.4$ is not as high initially, and after decreasing a bit it stabilizes higher than the acceptance rate for $k_BT/J = 1.0$. The fact that the acceptance rate for $k_BT/J = 1.0$ stabilizes faster than for $k_BT/J = 2.4$ is expected because we previously saw that it required less Monte Carly cycles to reach the most likely state for lower temperatures.

It is also expected that the acceptance rate for $k_BT/J = 1.0$ stabilizes at 0 because the probability for a new configuration to be accepted is given by the Boltzmann distribution, which is very low for low

temperatures. The same argument works for the stabilization of the acceptance rate for $k_BT/J = 2.4$. Here we have a higher temperature and therefore the probability for a new configuration to be accepted is higher.

5.3 Energy probability distribution

The strongly peaked energy distribution for the $k_BT/J = 1.0$ case in Figure 4, is a reflection of the previous results in Figure 1 and Figure 3. The energy stabilize after about 10^5 cycles, after which the acceptance rate is close to zero. Thus, the energy will stay close to the minima at $\langle E \rangle \approx -2.0$ for the vast amount of the simulation. For $k_BT/J = 2.4$, the energy stabilize after 10^6 cycles, but from Figure 3, we see that the acceptance rate does not go to zero over the number of cycles.

For the lower temperature, the conditional test in Metropolis is strongly inclined to decrease the temperature. While the condition is a lot less strict with $k_BT/J = 2.4$, and we get something closer to a Boltzmann distribution.

This is again confirmed in the variance plot in Figure 5. For both temperatures, the variance decrease over the cycles, as the energy stabilize. However, the decrease is steeper for $k_BT/J = 1.0$. After 10^7 cycles, the variance at $k_BT/J = 2.4$ is more than two orders of magnitude higher, reflecting the distribution functions in Figure 4.

5.4 Phase transitions

As the temperature approach the critical temperature, the expectation value for the energy start to increase, while the absolute magnetisation declines steeply. While it is hard to extinguish the behaviour of the different lattice sizes for the energy, the drop increase with lattice size for the magnetisation.

With the abrupt changes in energy and absolute magnetisation, their variances increase. This is manifested in the plots for C_V and χ in Figure 7. The behavior over lattice size can be tied back to Equation 5 and Equation 6. At temperature $T = T_C$, we expect broad maxima that narrows with lattice size. We see this clearly in Figure 7.

5.4.1 Parallelization

During the parallelized run we had a speedup of 2.73, while the theoretical speedup with 4 CPUs are 4. The reason we were a bit away from the theoretical results are probably that some of the computation power in the PC was being used to run other processes. For instance minor processes to keep the operating system up and so on.

The functionality of the parallelized code is not ideal. In the parallelized run, we run the same code as when not parallelized, but 4 times, and not once, 2.73 times faster as we would want. This means that if the original code was very slow, parallelizing it would not make much of an impact, since it would just use the same amount of time, or a bit more, to do it 4 times instead of doing it 1 time, 2.73 times faster.

5.5 Critical temperature for $L = \infty$

The critical temperature we found with our estimation was $T_C(L = \infty) \approx 2.42$, analytically this has been found by Lars Onsager[2] to be $T_C(L = \infty) \approx 2.269$. We are quite close to the analytical result, only 0.13 away.

Most of the uncertainty in our estimation probably comes from the reading of the critical temperature for different lattice sizes in the plots. Not all the plots, especially for low lattice sizes, had very distinct and clear critical temperatures. Another source for uncertainty comes from the stepsize which was $dT = 0.005$. This is assumed to be very small compared to the reading error, as we can't even tell one point in the plot from the next one.

6 Conclusion

We have successfully made an implementation of a 2-dimensional Ising model with square lattices with both ordered and random initial states. The model has been tested against known analytical quantities (see

appendix) for a 2×2-lattice with satisfactory precision. The model was also run on lattice sizes ranging from 20×20 to 100×100. In doing so we found the amount of Monte Carlo cycles needed in the Metropolis algorithm to reach the most likely state, which was 10^6 cycles.

In addition we have studied the acceptance rate of new configurations in the Metropolis algorithm as well as the probability distribution of energies on different temperatures. The results of this were the expected Boltzmann distribution that is used in the Metropolis algorithm.

We then used the model to study phase transitions by running the Metropolis algorithm on different lattices at different temperatures, resulting in the plots in Figure 6 and 7. Lastly these results was used to estimate the critical temperature in the thermodynamic limit as $L \to \infty$. The estimation lead to $T_C(L = \infty) \approx 2.42$ against the analytical value of $T_C(L = \infty) \approx 2.269$[2].

References

[1] Hjort-Jensen, M. Computational Physics. University of Oslo, 2015.

[2] Onsager, L. Crystal Statistics . I. A Two-Dimensional Model with an Order-Disorder Transition, Phys. Rev vol 65 p 117-149, 1944.

[3] https://www.open-mpi.org/software/ompi/v4.0/, May 2019

[4] https://en.cppreference.com/w/cpp/chrono, Nov 2019

A 2x2 lattice values

For a $L = 2$ lattice, there is $2^4 = 16$ possible states. The energies and magnetisations of these, can be calculated with Equations 1 and 2, resulting in the values below

# spins up	Degeneracy	Energy	Magnetization
4	1	-8J	4
3	4	0	2
2	4	0	0
2	2	8J	0
1	4	0	-2
0	1	-8J	-4

From this, we can calculate the partition function,

$$Z = \sum_{i=1}^{1} 6e^{-\beta E_i} = 2e^{8J\beta} + 2e^{-8J\beta} + 12e^{0\cdot\beta} = 4\cosh(8J\beta) + 12,$$

The expectation values

$$\langle E\rangle = \frac{1}{NZ}\sum_{i=1}^{1} 6E_i e^{-\beta E_i} = \frac{2(-8Je^{\beta 8J}) + 2(8Je^{-\beta 8J})}{(4\cosh(8J\beta) + 12)} = -\frac{8J\sinh(\beta 8J)}{\cosh(\beta 8J) + 3},$$

$$\langle E^2\rangle = \frac{1}{Z}\sum_{i=1}^{1} 6E_i^2 e^{-\beta E_i} = \frac{2(-8J)^2 e^{\beta 8J} + 2(8J)^2 e^{-\beta 8J}}{4\cosh(8J\beta) + 12} = \frac{64J^2\cosh(\beta 8J)}{\cosh(\beta 8J) + 3},$$

$$\langle|\mathcal{M}|\rangle = \frac{1}{Z}\sum_{i=1}^{1} 6|\mathcal{M}|_i e^{-\beta E_i} = \frac{4e^{\beta 8J} + 4e^{\beta 8J} + 2\cdot 4e^{0\cdot\beta} + 2\cdot 4e^{0\cdot\beta}}{4\cosh(8J\beta) + 12} = \frac{2e^{\beta 8J} + 4}{\cosh(8J\beta) + 3},$$

and

$$\langle\mathcal{M}^2\rangle = \frac{1}{Z}\sum_{i=1}^{1} 6\mathcal{M}_i^2 e^{-\beta E_i} = \frac{4^2 e^{\beta 8J} + (-4)^2 e^{\beta 8J} + 4\cdot 2^2 e^{0\cdot\beta} + 4\cdot(-2)^2 e^{0\cdot\beta}}{4\cosh(8J\beta) + 12} = \frac{8(e^{\beta 8J} + 1)}{\cosh(\beta 8J) + 3}.$$

From these, we get

$$C_V = \frac{1}{k_B T^2}(\langle E^2\rangle - \langle E\rangle^2) = \frac{1}{k_B T^2}\left[-\frac{64J^2\cosh(\beta 8J)}{\cosh(\beta 8J) + 3} - \frac{64J^2\sinh^2(\beta 8J)}{(\cosh(\beta 8J) + 3)^2}\right]$$

and

$$\chi = \frac{1}{k_B T}(\langle\mathcal{M}^2\rangle - \langle\mathcal{M}\rangle^2) = \frac{1}{k_B T}\left[\frac{8(e^{\beta 8J} + 2)}{\cosh(\beta 8J) + 3}\right]$$

Plugging in $J = T = k_B = \beta = 1$, the values per spin $L^2 = 4$ are

$\langle E\rangle$	$\langle\lvert\mathcal{M}\rvert\rangle$	C_V	χ
-1.995982	0.9986607	0.032085	0.004005